

1 **Mist Cannon Trucks Can Exacerbate the**
2 **Formation of Water-Soluble Organic Aerosol and**
3 **PM_{2.5} Pollution in the Road Environment**

4

5 Yu Xu¹, Xin-Ni Dong², Chen He³, Dai-She Wu⁴, Hong-Wei Xiao¹, Hua-Yun Xiao^{1,*}

6

7 ¹School of Environmental Science and Engineering, Shanghai Jiao Tong University,
8 Shanghai 200240, China

9 ²Jiangxi Province Science and Technology Information Institute, Nanchang 330000,
10 China

11 ³State Key Laboratory of Heavy Oil Processing, China University of Petroleum, Beijing
12 102249, China

13 ⁴School of Resource, Environmental and Chemical Engineering, Nanchang University,
14 Nanchang 330031, China

15

16

17

18 *Corresponding author: Hua-Yun Xiao

19 E-mail: xiaohuayun@sjtu.edu.cn

20 Phone: +86-173-0183-7060

21

22

23

24

25 **Abstract:** Mist cannon trucks have been widely applied in megacities in China to
26 reduce the road dust, since they are considered to be more water-saving and efficient
27 than the traditional sprinkling trucks. However, their effect on the formation of water-
28 soluble organic compounds and the pollution control of fine particle (PM_{2.5}) remains
29 unknown. We characterized the variations of chemical compositions in PM_{2.5} collected
30 on the road sides during the simulated operations of mist cannon truck and traditional
31 sprinkling truck via Fourier transform ion cyclotron resonance mass spectrometry and
32 ion chromatography. The mass concentrations of water-soluble organic carbon in PM_{2.5}
33 showed a significant increase (62–70%) after air spraying. Furthermore, we found that
34 water-soluble organic compounds, particularly organic nitrates, increased significantly
35 via the interactions of reactive gas-phase organics, atmospheric oxidants, and aerosol
36 liquid water after air spraying, although the air spraying had a better effect on
37 suppressing road dust than the ground aspersion. Moreover, the formation of PM_{2.5} on
38 the road segment where the mist cannon truck passed by was promoted, with an increase
39 of up to 13% in mass concentration after 25–35 minutes, on average. Thus, the
40 application of mist cannon trucks potentially worsens the road atmospheric
41 environment through the increase in PM_{2.5} levels and the production of a large number
42 of water-soluble organic compounds in PM_{2.5}. The overall results provide not only
43 valuable insights to the formation processes of water-soluble organic compounds
44 associated with aerosol liquid water in the road environment but also management
45 strategies to regulate the operation of mist cannon trucks in China.

46

47 **1 Introduction**

48 Over the past decade, the demand for effective road dust control has grown
49 dramatically due to the upgraded environmental protection policies. Traditionally, the
50 sprinkling trucks with the ground aspersion work well for vehicle-generated road dust.
51 The newly developed mist cannon trucks are able to spray water mist up to 120 m away
52 and 100 m high, with a droplet diameter of as small as 5 μm . They are considered to be
53 more water-saving and efficient than the traditional sprinkling trucks (the ground
54 aspersion), although the relevant argumentation work is rarely systematically studied.
55 In recent years, the mist cannon trucks have been widely utilized by the local
56 environmental bureau to achieve the target of strict emission control in megacities in
57 China (Wang et al., 2022). Traffic-related emissions contribute a huge amount of
58 volatile organic compounds (VOCs), nitrogen oxides (NO_x), ammonia (NH_3), and fine
59 particles ($\text{PM}_{2.5}$) to the urban atmosphere, which exerts adverse impacts on human
60 health and climate change (Yang et al., 2022; Deng et al., 2020). However, no study has
61 investigated whether and how the water mist sprayed by mist cannon truck affects the
62 road atmospheric environment.

63 The mist cannon trucks can spray a large amount of fine water mist in a short time,
64 hence the air humidity of local road environment where the mist cannon truck passed
65 by will increase sharply. Aerosol liquid water (ALW) exists in the condensed phase as
66 a function of gas and particle chemical composition, particle concentration, temperature
67 (T), and relative humidity (RH) (Xu et al., 2020b; Nguyen et al., 2015). Thus, an
68 increase in RH can promote the rise in ALW concentration (Guo et al., 2015). It is well

69 documented that ALW plays an important role in the formation of secondary organic
70 aerosol (SOA) via the partitioning of gas-phase water-soluble organics to the particle
71 phase and subsequent aqueous-phase reactions (Sareen et al., 2017; Carlton and Turpin,
72 2013). The severe haze episodes in Beijing can even be partly attributed to the
73 interactions between ALW (or high RH) and aerosol organic components (Li et al., 2019;
74 Wang et al., 2021). In particular, 40–80% of fossil-fuel-derived primary organic
75 aerosols were found to be water-soluble (Qiu et al., 2019). However, there are large
76 knowledge gaps in our current understanding on ALW-related organic compound
77 formation in the road environment with mist cannon truck operation.

78 Although few studies have systematically evaluated the ability of mist cannon
79 truck to remove road dust, it is easy to understand that the tiny water droplets generated
80 by mist cannon system can indeed capture coarse particles (i.e., dropping dust to the
81 ground) more effectively than the water column sprayed by the traditional sprinkling
82 truck. However, fine particles (PM_{2.5}) are commonly regarded as a major threat to urban
83 atmospheric environment and human health (Yue et al., 2020). Thus, assessing the
84 impact of mist cannon truck operation on road PM_{2.5} pollution is of great significance
85 for guiding future environmental protection initiatives.

86 In this study, we simulated the operation scenes of mist cannon truck and
87 traditional sprinkling truck on the sides of the urban road (Nanchang, eastern China).
88 We collected ambient PM_{2.5} samples in these scenes. The molecular compositions of
89 water-soluble organic matter (WSOM) in the collected samples were resolved using
90 ultrahigh-resolution Fourier transform ion cyclotron resonance mass spectrometry (FT-

91 ICR MS). Moreover, we also presented the measurement of other chemical components
92 (e. g., water-soluble ions) in PM_{2.5} samples and the predicted ALW concentration. The
93 concentrations of PM_{2.5} were also monitored on the road segment where the mist
94 cannon truck passed by. The overall results will shed light on the impact of spraying
95 water mist by mist cannon truck on the formation of water-soluble organic compound
96 and its implications for PM_{2.5} pollution control in the urban road environment for the
97 first time.

98

99 **2 Materials and methods**

100 **2.1 Study site and sample collection**

101 A branch road (provincial capital north 2nd road) located in the centre of Nanchang
102 (Eastern China) was selected as the study area (**Fig. 1a**). This area is characterized by
103 heavy traffic and high population density. There are no typical pollution sources, such
104 as factories and garbage treatment plants, within 30 km of the study area. The trees on
105 both sides of the road are very tall and lush (**Fig. 1a**), which makes the atmosphere in
106 this road environment relatively stable. The dominant tree species in this area are
107 camphor trees (*Cinnamomum Camphora*). Thus, the region is expected to be influenced
108 by both anthropogenic (e.g., vehicle exhausts) and biogenic VOCs.

109 Two sampling points (a distance of approximately 70 m) on the road side were
110 selected, which were affected by air spray and ground aspersion, respectively (**Fig. 1b–**
111 **e**). The air spraying at a height of 8 m above the ground was to simulate the water mist
112 sprayed by the mist cannon truck. In contrast, the ground aspersion with a height of 0.4
113 m above the ground was designed to simulate the operation of traditional sprinkling

114 truck. The residence time of the fine water mist sprayed by the mist cannon truck in the
115 air is assumed to be several minutes to tens of minutes, which mainly depends on the
116 ambient temperature, RH, and wind speed. As mentioned above, the lush trees on both
117 sides of the road cause the atmosphere in the road environment to be relatively stable.
118 Moreover, we found that each simulated air spray can maintain a high level of RH for
119 several minutes (about 4–8 minutes). Thus, the frequency of spraying water (Milli-Q
120 water, 18.2 MΩ cm) was set to 1 minute spraying every 8 minutes in this study. This
121 spraying operation can prevent the resuspension of road dust as much as possible. The
122 spraying was controlled by an intelligent timing irrigation equipment (Nadster, China).
123 The diameter of the pores in the nozzle for air spraying is less than 0.8 mm, while that
124 in the nozzle for ground aspersion is approximately 6 mm.

125 PM_{2.5} samples were collected onto prebaked (500°C for ~10 hours) quartz fiber
126 filters (Pallflex, Pall Corporation, USA) using a high-volume air sampler (Series 2031,
127 Laoying, China). Sampling at the above-mentioned two sites was simultaneously
128 performed from March 23 to March 26, 2021. The duration of each aerosol sampling
129 was approximately 4 h (9:00–13:00 LT) every day. We observed that the traffic flow on
130 March 25 was higher than that on other days. The weather during the sampling periods
131 from March 23 to March 26 was cloudy to sunny, sunny, sunny, and shower (only one
132 short precipitation event in the sampling period), respectively. The average ambient T
133 was approximately 21 °C. The average ambient RH in those periods (March 23–25)
134 ranged between 50% and 60%. The average RH can reach 84–87% after air spraying.
135 On March 26, the average ambient RH was as high as 80% during the period of 9:00–

136 13:00. Thus, the water spraying operation was stopped when the samples were collected
137 on March 26. All samples were stored at $-28\text{ }^{\circ}\text{C}$ prior to the analysis. In addition, the
138 mass concentrations of $\text{PM}_{2.5}$ were measured online (Thermo Scientific 5030i, USA)
139 from July to August 2021 near the trunk road where the mist cannon truck was
140 frequently operated (**Fig. 1a**). Typically, the mist cannon truck was operated back and
141 forth on specific road sections to prevent the resuspension of dust. Thus, the $\text{PM}_{2.5}$
142 online monitoring was performed after the misting cannon truck passed through the
143 monitoring point several times. Specifically, $\text{PM}_{2.5}$ concentrations near road (81 road,
144 Nanchang) were recorded at 5-minute intervals from 10 minutes before to 50 minutes
145 after the mist cannon truck passed by.

146

147 **2.2 Chemical analysis**

148 A portion of each filter sample was ultrasonically extracted with Milli-Q water
149 (MQW). WSOM in the extracting solution was further extracted using the previously
150 reported solid-phase extraction (SPE) method (Dittmar et al., 2008; Qiao et al., 2020;
151 Xie et al., 2020). Briefly, the cartridge (PPL, 0.5 g, Agilent) was rinsed with 18 mL of
152 methanol (LC-MS grade, Thermo Fisher) and 18 mL of HCl solution ($\text{pH} = 2$) in turn.
153 Subsequently, the extracts with acidity adjusting ($\text{pH} = 2$) were injected into a cartridge.
154 Acidified MQW (18 mL) and normal MQW (6 mL) were added in turn to remove the
155 salt and chloride ion trapped in the cartridge. After drying under a stream of N_2 , trapped
156 OM was eluted using 15 mL of methanol. The eluted solution was concentrated to 4 mL
157 and then preserved at $-28\text{ }^{\circ}\text{C}$ until analysis. The molecular compositions of WSOM in

158 PM_{2.5} samples were determined using a Bruker Apex Ultra Fourier transform ion
159 cyclotron resonance mass spectrometry (FT-ICR MS) (Bruker, Germany) coupled to an
160 Apollo II Electrospray ionization (ESI) (He et al., 2020). The samples were injected
161 into the ionization source at 250 $\mu\text{L h}^{-1}$ through a syringe pump. The instrument was
162 operated in the negative-ion mode. One hundred and twenty-eight continuous scans
163 were acquired in each analysis to increase the signal-to-noise ratio of the mass spectrum.
164 Blank was analyzed with the same procedure. Detailed methodologies and data quality
165 control have been described elsewhere (He et al., 2020; He et al., 2019).

166 Another filter cut was ultrasonically extracted with MQW for the determination of
167 water-soluble organic carbon (WSOC), water soluble total nitrogen (WSTN), and
168 inorganic ions. The mass concentrations of WSOC and WSTN in samples were
169 measured with a total organic carbon/total nitrogen analyser (Elementar vario, Germany)
170 (Xu et al., 2019). The mass concentration of WSOC was converted to that of WSOM
171 using a conversion factor of 1.8 (Müller et al., 2017; Finessi et al., 2012; Yttri et al.,
172 2007; Simon et al., 2011). The mass concentrations of water-soluble inorganic ions,
173 such as SO_4^{2-} , NO_3^- , NH_4^+ , and K^+ , were measured using an ion chromatography
174 system (Dionex, Thermo, USA) (Xu et al., 2020a; Xu et al., 2022). The mass
175 concentration of water-soluble organic nitrogen (WSON) was calculated as the
176 difference in the concentrations between WSTN and inorganic nitrogen (i.e., $\text{NO}_3^- \text{N}$
177 + $\text{NO}_2^- \text{N}$ + $\text{NH}_4^+ \text{N}$) (Xu et al., 2020b). Ambient T and RH were measured using a
178 temperature and humidity monitor (CEM 9880M, China).

179

180 **2.3 Compound categorization and ALW prediction**

181 The molecular formulas assigned from FT-ICR MS were classified into four main
182 compound groups in this study. These identified groups include CHO (containing only
183 C, H, and O), CHON (containing C, H, O, and N), CHOS (containing C, H, O, and S),
184 and CHONS (containing C, H, N, O, and S) (Song et al., 2018). The double-bond
185 equivalent (DBE) was calculated to describe the unsaturation degree of the organic
186 compounds (see details in **Sect. S1** in the Supplement) (Schmidt et al., 2017; Qiao et
187 al., 2020). The modified aromaticity index (AI_{mod}) was calculated to reflect the
188 aromaticity of organic molecules (see details in **Sect. S1** in the Supplement) (Schmidt
189 et al., 2017; Koch and Dittmar, 2006). The carbon oxidation state (OSc) was used to
190 indicate the evolving composition of aerosol organics that underwent oxidation
191 processes (Kroll et al., 2011). The details of OSc calculation were shown in **Sect. S1** in
192 the Supplement. According to the oxygen-to-carbon (O/C) and hydrogen-to-carbon
193 (H/C) elemental ratios, the identified molecular formulas were further classified into
194 five compound categories, including unsaturated aliphatic-like (UA), highly
195 unsaturated-like (HU), highly aromatic-like (HA), polycyclic aromatic-like (PA), and
196 saturated-like (Sa) molecules (Su et al., 2021). These classified compound categories
197 were visualized in the van Krevelen diagram (see details in **Sect. S1** in the Supplement).

198 The thermodynamic model ISORROPIA-II was applied to calculate the mass
199 concentrations of ALW driven by inorganic components (Guo et al., 2015; Tan et al.,
200 2017; Xu et al., 2022). The model predicts the inorganic ALW based on the mass
201 concentrations of inorganic species, RH, and T (see details in **Sect. S2** in the

202 Supplement). Particle hygroscopicity is also influenced by organics in aerosol particles
203 (Sareen et al., 2013; Cruz and Pandis, 2000). The impact of organic fraction on aerosol
204 water is complex and depends on the composition of organic matter (Nguyen et al.,
205 2016). In this study, the mass concentration of water associated with aerosol organic
206 fraction was predicted according to the previously reported method (see details in Sect.
207 S2 in the Supplement) (Nguyen et al., 2016; Nguyen et al., 2015).

208

209 **3 Results and discussion**

210 **3.1 Chemical characteristics of PM_{2.5} in different road segments**

211 **Figure 2** compares the differences in the chemical composition of PM_{2.5} collected
212 in the air spray road segment and ground aspersion road segment. The mass fraction of
213 WSOM was the highest regardless of the weather and road section where the samples
214 were collected, which accounted for 30–40% of the total water-soluble components
215 (**Fig. 2a–d**). From March 23 to March 25, the mass concentrations and fractions of
216 WSOM (/WSOC) were higher on the air spray road segment than on the ground
217 aspersion road segment. For the case without water spray treatment (as reference group),
218 the chemical compositions of PM_{2.5} samples collected from those two adjacent road
219 segments only showed small differences in concentration (**Fig. 2d, h, i**). It suggested
220 that the impact of background PM_{2.5} or meteorological factor on PM_{2.5} composition or
221 level was similar between these two study sites. Obviously, the variations in the mass
222 concentrations and fractions of WSOM from the air spray road segment to the ground
223 aspersion road segment can be attributed to the differences in water-soluble SOA yield

224 or formation pathway caused by different water spray treatments.

225 The mass concentrations of ALW, WSOC, and WSON tended to decrease from the
226 air spray road segment to the ground aspersion road segment (**Fig. 2e–g**). Moreover,
227 linear regression analysis showed that the mass concentrations of ALW ($n = 8$) were
228 significantly positively ($P < 0.01$) correlated with those of WSOC and WSON, with the
229 R^2 values of 0.84 and 0.75, respectively. The results were consistent with those obtained
230 by previous studies conducted in an agriculture area in Italy (Hodas et al., 2014) and a
231 suburban forest site in Tokyo (Xu et al., 2020b). Moreover, these studies by Hodas et
232 al. (2014) and Xu et al. (2020b) suggested that the ALW dependence of reactive gas
233 uptake and subsequent aqueous reactions significantly contributed the production of
234 WSOC and WSON. Thus, the increase in ALW concentration after air spraying can
235 promote the formation of water-soluble organic compounds in $PM_{2.5}$ in the road
236 environment.

237 Nitrate and sulfate were the most abundant inorganic components (**Fig. 2a–d**),
238 which have been identified as typical factors controlling ALW (Hodas et al., 2014).
239 From the air spray road segment to the ground aspersion road segment, the decrease in
240 nitrate concentration was more significant than that in sulfate concentration (**Fig. 2i–**
241 **k**). Moreover, the concentration of nitrate significantly correlated with that of ALW (P
242 < 0.01 , $R^2 = 0.7$). In contrast, the sulfate did not show a strong correlation with ALW
243 ($R^2 = 0.3$). As we know, the gas-phase oxidation of NO_2 by hydroxyl radical ($\bullet OH$) to
244 form nitric acid (HNO_3) is an important pathway for the formation of daytime nitrate
245 aerosol (Fu et al., 2020; Chen et al., 2020). Hydroxyl radical can be rapidly produced

246 by O₃ photolysis under conditions with abundant water vapour and sunlight (as in this
247 study) (Li et al., 2022), which is undoubtedly beneficial to the production of HNO₃.
248 Thus, in the region with large NO_x and ammonia emissions (originated from vehicle
249 exhausts (Yang et al., 2022)), the formation of daytime nitrate aerosol could be
250 promoted by enhanced RH (24–43% of increase) after air spraying. This is also partly
251 supported by the thermodynamics of ammonium nitrate formation (Mozurkewich, 1993;
252 Hodas et al., 2014). Additionally, it has been suggested that the formation of nitrate and
253 ALW is mutually reinforcing (Chen et al., 2022). Thus, the increase in ALW
254 concentration after air spraying was mainly driven by RH and locally (traffic emissions)
255 formed nitrate aerosol.

256 Interestingly, Ca²⁺ and Mg²⁺ showed a significant increase in concentration from
257 the air spray road segment to the ground aspersion road segment (**Fig. 2i–k**), which was
258 contrary to the case of other components (e.g., WSOC, ALW, and nitrate). In addition,
259 during March 26 without water spray treatment, the differences in both Ca²⁺ and Mg²⁺
260 concentrations between those two adjacent road segments were almost negligible (**Fig.**
261 **2l**). It is well known that Ca²⁺ and Mg²⁺ are typical crustal materials and are mainly
262 enriched in atmospheric coarse particles (Chen and Chen, 2008). Thus, a decrease in
263 Ca²⁺ and Mg²⁺ concentrations after air spraying implied that the water mist sprayed by
264 mist cannon truck had a better effect on suppressing road dust than the ground aspersion
265 by traditional sprinkling truck.

266

267 **3.2 Molecular characteristics of water-soluble organic compounds**

268 Thousands of molecular formulas (5966–8102) were observed in WSOM in PM_{2.5}
269 collected from road environment (**Table 1**). The CHO molecular formulas (1089–2037)
270 accounted for 20–25% in all molecular formulas. Further, CHO compounds were
271 classified according to the number of oxygen atoms in their molecules. The subgroups
272 ranged from O₂ to O₁₅ (**Fig. 3**). The number and intensity of dominated O₅–O₁₀
273 subgroups accounted for 72–85% and 71–86% of the total compounds, respectively;
274 moreover, these percentages were higher than the results reported for aerosols in Beijing
275 (Xie et al., 2020). The average H/C and O/C ratios of CHO compounds varied from
276 1.08 to 1.24 and from 0.42 to 0.49, respectively (**Table S1**). The average O/C ratios
277 were higher than the value (0.33 ± 0.11) obtained from urban aerosols (Beijing, China),
278 while the H/C ratios showed relatively small differences between our results and
279 observation results in Beijing (1.14 ± 0.37) (Xie et al., 2020). In addition, another study
280 performed in Beijing showed that the average O/C and H/C ratios of organic aerosols
281 were in the range of 0.47–0.53 and 1.52–1.63, respectively (Hu et al., 2017). These
282 dissimilarities might be attributed to the fact that the sources of urban aerosols are more
283 complex than those of aerosols collected from road environments.

284 The average H/C and O/C ratios of CHON compounds ranged from 1.05 to 1.21
285 and 0.42 to 0.51, respectively (**Table S1**). The H/C ratio ranges of CHON compounds
286 in this study overlapped with those measured in previous studies (Su et al., 2021; Xie
287 et al., 2020). However, the O/C ratios of CHON compounds were relatively higher in
288 road-derived aerosols than in aerosols (0.36 ± 0.12) or snow (0.32–0.37) collected in
289 urban areas (building roof) (Su et al., 2021; Xie et al., 2020). This difference might be

290 associated with the influence of source strength (e.g., vehicle exhausts) and atmospheric
291 oxidation capacity. The number of CHON formulas (1501–2685) was much higher than
292 that of CHO formulas (**Table 1**). The assigned CHON formulas were further divided
293 into CHON₁ (N₁O₂–N₁O₁₆), CHON₂ (N₂O₂–N₂O₁₃), and CHON₃ (N₃O₂–N₃O₁₃) groups
294 (**Fig. 3**). CHON₁ was found to be the dominant nitrogen-containing species in all
295 samples, which was consistent with previous reports on urban aerosols and snow (Su et
296 al., 2021; Xie et al., 2020). Moreover, the CHON₁ compounds with O/N > 2 contributed
297 99.2–100.0% to total CHON₁ species in all samples. The CHON₂ compounds with O/N >
298 2 accounted for 90.2–100.0% of total CHON₂ species. For CHON₃ group, the
299 proportion of nitrogen-containing compounds with O/N > 2 was 53.0–61.8%. The
300 CHON species with O/N > 2, which allows an assignment of oxidized-form nitrogen,
301 are preferentially ionized in negative electrospray ionization mode (Lin et al., 2015; Su
302 et al., 2021). Studies on the compositions of organic matter in urban rainwater and
303 aerosols have suggested that numerous CHON compounds contained oxidized nitrogen
304 function groups (e.g., –ONO₂) and that NO_x-related oxidation processes can be
305 responsible for the formation of these CHON compounds (Altieri et al., 2009; Lee et
306 al., 2016). Thus, the CHON compounds with O/N > 2 in our PM_{2.5} samples can be
307 assumed to be mostly in an oxidized form (e.g., organic nitrates).

308 **Figure 3** also shows the differences in the number of CHO and CHON species
309 between the air spray road segment and ground aspersion road segment. The abundance
310 of each O_n subgroup in CHO compounds considerably enhanced after air spraying,
311 especially the subgroups of O₅–O₁₁. In contrast, the number of CHO species for these

312 two cases without water spray treatment showed a smaller difference (**Fig. 3d**). In
313 general, the total number of CHO compounds increased significantly after air spraying
314 (**Fig. 3** and **Table 1**). However, there was no significant change for the total number of
315 CHO species between the two cases without water spray treatment. These findings
316 implied that the increased ALW after air spraying can substantially contribute to the
317 formation of CHO compounds with a more oxygenated state.

318 The number of CHON compounds decreased significantly from the air spray road
319 segment to the ground aspersion road segment, a variation pattern of which was similar
320 to that of CHO compounds (**Fig. 3** and **Table 1**). Furthermore, the decrease in the
321 number of molecules from the air spray road segment to the ground aspersion road
322 segment was more remarkable for CHON₁ compounds than for CHON₂ compounds. In
323 contrast, the variation in the number of CHON₃ molecules after air spraying was less
324 significant than that of CHON₁₋₂ compounds. In addition, insignificant change in the
325 number of CHON compounds was found in PM_{2.5} collected in the two road segments
326 without water spray (**Fig. 3d**). Thus, the increase in the number of nitrogen-containing
327 compounds after air spraying indicated that the interactions among ALW, traffic-
328 derived reactive nitrogen, and ambient VOCs may play an important role in organic
329 nitrogen compound formation in PM_{2.5}. This consideration can also be partly supported
330 by the result obtained by Xu et al. (2020b) in a suburban forest in Tokyo, Japan. The
331 authors suggested that ALW is a key promoter for the formation of aerosol WSON
332 through secondary processes associated with atmospheric reactive nitrogen and
333 biogenic VOCs (Xu et al., 2020b). For sulfur-containing compounds, their molecular

334 numbers just showed a relatively small change after air spraying (**Fig. S1**). This
335 suggested that the impact of ALW on sulfur-containing compound formation was
336 weaker than that of ALW on the formation of CHO and CHON compounds in this road
337 environment.

338

339 **3.3 CHO and CHON species formed under the influence of increased ALW**

340 The molecular compositions of CHO compounds in PM_{2.5} in the van Krevelen
341 diagram were scattered across wider ranges in the air spray road segment than in the
342 ground aspersion road segment, particularly in the sunny days (March 24 and March
343 25) (**Fig. 4**). Moreover, common CHO molecules accounted for 39% (sunny day) – 63%
344 (cloudy to sunny day) and 90–95% of CHO molecules in PM_{2.5} collected from the air
345 spray and ground aspersion road segments, respectively (**Table 1**). In contrast, common
346 CHO molecules contributed 81–85% of CHO molecules in PM_{2.5} collected from two
347 road segments without water spray (I and II). These results can be explained by the
348 increased molecular diversity caused by ALW-related atmospheric processes. It also
349 implied the importance of photochemical reactions in CHO compound formation.
350 Furthermore, the unique CHO compounds were identified between PM_{2.5} samples in
351 the air spray road segment (/no water spray road segment (I)) and the ground aspersion
352 road segment (/no water spray road segment (II)) (**Fig. S2**). On March 23 and March
353 24, the newly emerging CHO compounds after air spraying were dominated by
354 unsaturated aliphatic-like and highly unsaturated-like compounds. However, both
355 unsaturated-like species (unsaturated aliphatic-like and highly unsaturated-like) and

356 aromatic-like species (highly aromatic-like and polycyclic aromatic-like) contributed
357 significantly to the newly emerging CHO compounds after air spraying on March 25
358 when the ALW and traffic flow were higher than other days (**Fig. S2**). Obviously, the
359 formation of those unique CHO compounds was closely associated with increased ALW.

360 **Figure 5** shows the OSc values of the identified unique CHO molecules. The OSc
361 values of these CHO molecules were higher than those of primary vehicle exhausts (–
362 2.0 to –1.9) (Aiken et al., 2008). The OSc values of the secondary organic aerosol
363 formed via the reactions of anthropogenic and biogenic VOCs (e.g., isoprene,
364 monoterpene, toluene, alkane, and alkene) and oxidants (e.g., O₃ and/or •OH) varied
365 from –1.1 to +1.0 (Kroll et al., 2011; Li et al., 2021b), which was within the OSc value
366 ranges of CHO molecules measured in this study. In addition, hydrocarbon-like organic
367 aerosol (HOA) likely linked with primary vehicle exhausts (Sun et al., 2016) only
368 accounted for less than 6% of total unique CHO compounds (**Fig. 5**). Although it is
369 difficult to classify all CHO molecules in **Fig. 5**, these identified unique CHO molecules
370 can at least suggest that the water mist from air spraying can promote the formation of
371 CHO compounds and increase their molecular diversity. As mentioned previously, there
372 are dense trees on both sides of the road. Thus, these newly emerging CHO compounds
373 can be largely attributed to secondary processes associated with the oxidation of vehicle
374 exhausts and biogenic VOCs by O₃ and/or •OH. In addition, we also observed increased
375 oligomerization (e.g., methylglyoxal (C₃H₄O₂) to form oligomers (C_{4–7}H_{6–10}O₅) in
376 particle phase) of CHO compounds after air spraying (Ma et al., 2022), particularly on
377 March 25 with a high ALW level and a large traffic flow (**Fig. S3c**). The overall results

378 implied that the water mist sprayed by mist cannon trucks can indeed enhance the
379 abundance and diversity of CHO compounds in PM_{2.5} via promoting gas-to-particle
380 partitioning of gas-phase oxidation products of VOCs and subsequent aqueous-phase
381 reactions.

382 For CHON compounds, their molecular compositions were scattered across an
383 increased range in the van Krevelen diagram after air spraying compared to the
384 observations in the ground aspersion case (**Fig. S4**). This was also indicated by the
385 relatively low proportion of common CHON molecules (45–55%) in total CHON
386 compounds for the cases with air spraying treatment (**Table 1**). Moreover, these newly
387 emerging CHON molecules after air spraying showed a high diversity, as shown in **Fig.**
388 **S5**. The group of CHON₁ was the dominant nitrogen-containing compound in the
389 identified unique CHON compounds. On March 23 and March 24, the main unique
390 CHON compounds emerged during air spraying were unsaturated aliphatic-like and
391 highly unsaturated-like nitrogen-containing species. The number of highly aromatic-
392 like and polycyclic aromatic-like compounds that newly emerged also increased
393 significantly following increased traffic flow and ALW (March 25). The results
394 suggested that the increase in ALW concentration after air spraying can facilitate the
395 formation of particle-phase nitrogen-containing compounds (Hallquist et al., 2009; Xu
396 et al., 2020b).

397 Organic nitrates have been supposed to be abundant in our PM_{2.5} samples collected
398 from road environment. It is well documented that atmospheric organic nitrates are
399 primary, secondary, and tertiary byproducts of reactions among anthropogenic and

400 biogenic VOCs, atmospheric oxidants (e.g., O₃, •OH, and nitrate radicals), and NO_x
401 (Lee et al., 2016; Yeh and Ziemann, 2014; Su et al., 2021). In addition, numerous
402 organic nitrates are known as semivolatile compounds, which are able to partition
403 between the gas and particle phases when they are oxidized or photolyzed (Bean and
404 Hildebrandt Ruiz, 2016). Recently, an oxidation and hydrolysis mechanism associated
405 with the formation of atmospheric organic nitrates has been proposed to interpret the
406 potential origins or precursors of CHON compounds (Su et al., 2021). In this study, we
407 found that 68–82% of newly emerging CHON₁ compounds after air spraying can be
408 explained by oxidation (e.g., R₁OH)-product (e.g., R₁ONO₂) pair proposed by Su et al.
409 (2021) (**Fig. 6a–c**). It indicated that these newly emerging CHON₁ compounds after air
410 spraying were largely derived from the transformation of CHO species under existence
411 of NO_x. A similar pattern was also observed in the newly emerging CHON₂ compounds
412 (**Fig. S6**). It should be pointed out that vehicle exhausts and roadside vegetation are
413 important sources for VOCs and NO_x in this road environment. However, the number
414 of unique CHON₁ and CHON₂ compounds identified in the comparative cases without
415 water spray treatment was much less than that identified in the comparative cases with
416 air spraying and ground aspersion treatments (**Fig. 6** and **Fig. S6**). In particular, we did
417 not observe significant oligomerization of CHON compounds after air spraying (**Fig.**
418 **S7**). Thus, these results suggested that the increase in ALW caused by air spraying can
419 facilitate the formation of organic nitrates via CHO compounds as potential precursors
420 under the presence of NO_x.

421

422 3.4 Environmental implication

423 Mist cannon sprayers are commonly applied in agriculture for the distribution of
424 fertilizers, pesticides, and herbicides. In recent years, misting cannon trucks are widely
425 developed and regraded as an excellent option for road dust control due to the
426 production of tiny water droplets that can drop dust to the ground. In particular, it is a
427 high-performance system of spraying disinfection in the road environment during the
428 COVID-19 epidemic period. For the first time, we provide a detailed characterization
429 of chemical compositions in road-derived PM_{2.5} under the influence of air spraying.
430 Recent study conducted in a rural site (Shanghai, China) has suggested that gaseous
431 water-soluble organic compounds mainly partitioned to the organic phase (organic shell)
432 under the condition of RH less than 80% (relatively low ALW) but to ALW under the
433 humid condition (RH > 80%, as air spraying operation), highlighting the importance of
434 high ALW in SOA formation processes (Lv et al., 2022). This is because aerosols can
435 exist in a phase-separated form with an inorganic core and an organic shell (Yu et al.,
436 2019; Li et al., 2021a; Ushijima et al., 2021). Our results verified the formation of
437 numerous unique CHO and CHON compounds by ALW-related promoting effect (**Fig.**
438 **7**). In particular, the mass concentrations of WSOC in PM_{2.5} increased by 62–70% after
439 air spraying. Clearly, although the air spraying by mist cannon system could exert a
440 better effect on suppressing road dust than the ground aspersion, as discussed previously,
441 air pollution induced by increased water-soluble organic compounds in PM_{2.5} will be
442 exacerbated in the road environment.

443 To reveal the influence of air spraying on PM_{2.5} pollution on the roadside, we

444 investigated the time series of percentage variation in road PM_{2.5} mass concentration
445 after the mist cannon truck was operated at a low-speed (< 30 km h⁻¹) (**Fig. 8**). It should
446 be pointed out that the mist cannon truck was usually operated back and forth on
447 specific road sections to prevent the resuspension of dust. After the misting cannon
448 truck passed through the monitoring site several times, repeated online PM_{2.5}
449 monitoring ($n = 34$, within a month) was performed to exclude the impact of dispersion
450 and traffic flow on analysis results. Accordingly, the resuspension of road dust was
451 expected to exert a relatively minor impact on the PM_{2.5} level near road. The
452 concentration of PM_{2.5} showed an increasing trend after the mist cannon truck passed
453 through the monitoring point for 15 minutes. Thus, the water droplets sprayed by the
454 mist cannon truck cannot directly cause an increase in PM_{2.5} concentration, suggesting
455 that the increased PM_{2.5} should be secondarily formed after water mist spraying (~15
456 minutes). This consideration was also supported by a significant increase in the
457 concentration and number of water-soluble organic compounds after air spraying (**Fig.**
458 **2** and **Fig. 3**). After the mist cannon truck has passed for 25–35 minutes, the increase
459 proportion of PM_{2.5} concentration on the roadside gradually reached the maximum
460 (~13%, on average). Subsequently, the proportion of increase in PM_{2.5} concentration
461 gradually decreased, reaching ~6% at 50 min after the mist cannon truck was operated.
462 In addition, the width of the road segment (81 road, Nanchang, China) where PM_{2.5} was
463 monitored is very large (~43 m), implying that the water mist sprayed by mist cannon
464 truck should exert a greater promoting effect on the formation of PM_{2.5} on conventional
465 urban roads. The overall results suggested that mist cannon truck cannot effectively

466 reduce the PM_{2.5} level in the road environment, but lead to aggravation of PM_{2.5}
467 pollution.

468 The chemical composition of fine aerosol particles in the urban road atmosphere
469 is highly complex, including a lot of harmful organic compounds (e.g., polycyclic
470 aromatic hydrocarbons and nitro-aromatics), as indicated by our measurements and
471 previous study (Tong et al., 2016). Emissions from vehicles and roadside vegetation are
472 important anthropogenic and biogenic sources of reactive gas-phase OC and key
473 precursors to form SOA in urban areas (Gentner et al., 2012; Xu et al., 2020b; Tong et
474 al., 2016). In particular, organic aerosol composition in the road environment can be
475 strongly impacted by vehicle emissions (e.g., VOCs and NO_x) (Tong et al., 2016).
476 Inhalation of the particles containing harmful organics can be responsible for a number
477 of adverse health effects (Künzli et al., 2000). However, the wide application of mist
478 cannon truck by local environmental protection department undoubtedly accelerates the
479 formation processes of water-soluble organic compounds and PM_{2.5}, which will further
480 worsen the urban road environment and cause health hazards to walking residents. Thus,
481 the present study provides the crucial information for the decision makers to regulate
482 the mist cannon truck operation in many cities in China.

483

484 **4 Conclusions**

485 We investigated the changes in the chemical composition of PM_{2.5} collected from
486 the road sides of the urban road during the simulated operations of mist cannon truck
487 and traditional sprinkling truck. Moreover, we also conducted online measurement of

488 PM_{2.5} concentration in the urban road segment where the mist cannon truck passed by.
489 The mass concentrations of WSOC in PM_{2.5} increased significantly (62–70%) from the
490 ground aspersion road segment to the air spray road segment. Similarly, ALW also
491 showed a significant increase after air spraying. We found that the mass concentration
492 of ALW in PM_{2.5} was significantly positively correlated with that of WSOC and WSON.
493 Thus, the increase of ALW after air spraying can promote the formation of particle-
494 phase water-soluble organic compounds in the road environment. In addition, the
495 decrease in Ca²⁺ and Mg²⁺ concentrations after air spraying suggested that the water
496 mist sprayed by mist cannon truck has a better effect on suppressing road dust than the
497 ground aspersion by traditional sprinkling truck.

498 A comparison in the number of CHO and CHON species between the air spraying
499 and ground aspersion road segments suggested that the increase in ALW after air
500 spraying can enhance the abundance and diversity of CHO and CHON compounds in
501 PM_{2.5}. The unique CHO compounds formed after air spraying can be largely attributed
502 to secondary processes associated with the oxidation of vehicle exhausts and biogenic
503 VOCs by oxidants and the oligomerization of CHO compounds. Organic nitrates were
504 considered to be the abundant nitrogen-containing compounds in PM_{2.5}. Furthermore,
505 we found that the increased organic nitrates were largely derived from the
506 transformation of CHO species under the existence of NO_x.

507 After the mist cannon truck has passed for 25–35 minutes, PM_{2.5} concentration on
508 the road side increased by up to 13%, on average. The proportion of increase in PM_{2.5}
509 concentration gradually decreased to ~6% at 50 min after the mist cannon truck was

510 operated. The overall results suggested that although mist cannon truck could suppress
511 road dust better than the traditional sprinkling truck, air pollution induced by increased
512 aerosol water-soluble organic compounds and PM_{2.5} levels will be exacerbated in the
513 urban road environment. Our findings provide new insights into the formation
514 processes of aerosol water-soluble organic compounds associated with the water mist
515 sprayed by mist cannon truck in the road atmospheric environment.

516

517 **Data Availability.** The data presented in this work are available upon request from the
518 corresponding authors.

519

520 **Supplement.** The supplement related to this article is available online at:
521 <https://doi.org/10.5194/acp-2022-735>.

522

523 **Author contributions.** YX, H-Y.X, and DW designed the study; YX, XD and H-W.X
524 performed field measurements; YX and CH performed chemical analysis and data
525 analysis; YX wrote the original manuscript; and YX reviewed and edited the manuscript.

526

527 **Competing interests.** The authors declare no competing financial interest.

528

529 **Disclaimer.** Publisher's note: Copernicus Publications remains neutral with regard to
530 jurisdictional claims in published maps and institutional affiliations.

531

532 **Acknowledgements.** The authors are very grateful to Chen-Xi Li for his kind and
533 valuable comments to improve the manuscript. Yu Xu acknowledges the Shanghai
534 Sailing Program (grant no. 22YF1418700) and the Natural (Youth) Science Foundation
535 of Jiangxi, China (grant no. 20212BAB213039).

536

537 **Financial support.** This research has been supported by the Shanghai Sailing Program
538 (grant no. 22YF1418700) and the Natural (Youth) Science Foundation of Jiangxi, China
539 (grant no. 20212BAB213039).

540

541 **Review statement.** This paper was edited by Annele Virtanen and reviewed by two
542 anonymous referees.

543

544 **References**

545 Aiken, A. C., DeCarlo, P. F., Kroll, J. H., Worsnop, D. R., Huffman, J. A., Docherty, K.
546 S., Ulbrich, I. M., Mohr, C., Kimmel, J. R., Sueper, D., Sun, Y., Zhang, Q.,
547 Trimborn, A., Northway, M., Ziemann, P. J., Canagaratna, M. R., Onasch, T. B.,
548 Alfarra, M. R., Prevot, A. S. H., Dommen, J., Duplissy, J., Metzger, A.,
549 Baltensperger, U., and Jimenez, J. L.: O/C and OM/OC Ratios of Primary,
550 Secondary, and Ambient Organic Aerosols with High-Resolution Time-of-
551 Flight Aerosol Mass Spectrometry, *Environ. Sci. Technol.*, 42, 4478-4485,
552 10.1021/es703009q, 2008.

553 Altieri, K. E., Turpin, B. J., and Seitzinger, S. P.: Oligomers, organosulfates, and

554 nitrooxy organosulfates in rainwater identified by ultra-high resolution
555 electrospray ionization FT-ICR mass spectrometry, *Atmos. Chem. Phys.*, 9,
556 2533-2542, 10.5194/acp-9-2533-2009, 2009.

557 Bean, J. K. and Hildebrandt Ruiz, L.: Gas-particle partitioning and hydrolysis of
558 organic nitrates formed from the oxidation of α -pinene in environmental
559 chamber experiments, *Atmos. Chem. Phys.*, 16, 2175-2184, 10.5194/acp-16-
560 2175-2016, 2016.

561 Carlton, A. and Turpin, B.: Particle partitioning potential of organic compounds is
562 highest in the Eastern US and driven by anthropogenic water, *Atmos. Chem.*
563 *Phys.*, 13, 10203-10214, 2013.

564 Chen, H. Y. and Chen, L. D.: Importance of anthropogenic inputs and continental-
565 derived dust for the distribution and flux of water-soluble nitrogen and
566 phosphorus species in aerosol within the atmosphere over the East China Sea, *J.*
567 *Geophys. Res.: Atmos.*, 113, D11. DOI: 10.1029/2007JD009491., 2008.

568 Chen, X., Wang, H., Lu, K., Li, C., Zhai, T., Tan, Z., Ma, X., Yang, X., Liu, Y., Chen,
569 S., Dong, H., Li, X., Wu, Z., Hu, M., Zeng, L., and Zhang, Y.: Field
570 Determination of Nitrate Formation Pathway in Winter Beijing, *Environmental*
571 *Science & Technology*, 54, 9243-9253, 10.1021/acs.est.0c00972, 2020.

572 Chen, Y., Wang, Y., Nenes, A., Wild, O., Song, S., Hu, D., Liu, D., He, J., Hildebrandt
573 Ruiz, L., Apte, J. S., Gunthe, S. S., and Liu, P.: Ammonium Chloride Associated
574 Aerosol Liquid Water Enhances Haze in Delhi, India, *Environ. Sci. Technol.*,
575 10.1021/acs.est.2c00650, 2022.

576 Cruz, C. N. and Pandis, S. N.: Deliquescence and hygroscopic growth of mixed
577 inorganic– organic atmospheric aerosol, *Environ. Sci. Technol.*, 34, 4313-4319.
578 <https://doi.org/4310.1021/es9907109>, 2000.

579 Deng, F., Lv, Z., Qi, L., Wang, X., Shi, M., and Liu, H.: A big data approach to
580 improving the vehicle emission inventory in China, *Nat. Commun.*, 11, 2801,
581 [10.1038/s41467-020-16579-w](https://doi.org/10.1038/s41467-020-16579-w), 2020.

582 Dittmar, T., Koch, B., Hertkorn, N., and Kattner, G.: A simple and efficient method for
583 the solid-phase extraction of dissolved organic matter (SPE-DOM) from
584 seawater, *Limnol. Oceanogr.: Meth.*, 6, 230–235, 2008.

585 Finessi, E., Decesari, S., Paglione, M., Giulianelli, L., Carbone, C., Gilardoni, S., Fuzzi,
586 S., Saarikoski, S., Raatikainen, T., and Hillamo, R.: Determination of the
587 biogenic secondary organic aerosol fraction in the boreal forest by NMR
588 spectroscopy, *Atmos. Chem. Phys.*, 12, 941-959. [https://doi.org/910.5194/acp-](https://doi.org/910.5194/acp-5112-5941-2012)
589 [5112-5941-2012](https://doi.org/910.5194/acp-5112-5941-2012), 2012.

590 Fu, X., Wang, T., Gao, J., Wang, P., Liu, Y., Wang, S., Zhao, B., and Xue, L.: Persistent
591 Heavy Winter Nitrate Pollution Driven by Increased Photochemical Oxidants in
592 Northern China, *Environmental Science & Technology*, 54, 3881-3889,
593 [10.1021/acs.est.9b07248](https://doi.org/10.1021/acs.est.9b07248), 2020.

594 Gentner, D. R., Isaacman, G., Worton, D. R., Chan, A. W. H., Dallmann, T. R., Davis,
595 L., Liu, S., Day, D. A., Russell, L. M., Wilson, K. R., Weber, R., Guha, A.,
596 Harley, R. A., and Goldstein, A. H.: Elucidating secondary organic aerosol from
597 diesel and gasoline vehicles through detailed characterization of organic carbon

598 emissions, *P. Natl. Acad. Sci. U. S. A.*, 109, 18318-18323,
599 doi:10.1073/pnas.1212272109, 2012.

600 Guo, H. Y., Xu, L., Bougiatioti, A., Cerully, K. M., Capps, S. L., Hite Jr, J., Carlton, A.,
601 Lee, S. H., Bergin, M., and Ng, N.: Fine-particle water and pH in the
602 southeastern United States, *Atmos. Chem. Phys.*, 15, 5211-5228.
603 <https://doi.org/5210.5194/acp-5215-5211-2015>, 2015.

604 Hallquist, M., Wenger, J. C., Baltensperger, U., Rudich, Y., Simpson, D., Claeys, M.,
605 Dommen, J., Donahue, N., George, C., and Goldstein, A.: The formation,
606 properties and impact of secondary organic aerosol: current and emerging issues,
607 *Atmos. Chem. Phys.*, 9, 5155-5236, 2009.

608 He, C., Pan, Q., Li, P., Xie, W., He, D., Zhang, C., and Shi, Q.: Molecular composition
609 and spatial distribution of dissolved organic matter (DOM) in the Pearl River
610 Estuary, China, *Environ. Chem.*, 17, 10.1071/EN19051, 2019.

611 He, C., Zhang, Y., Li, Y., Zhuo, X., Li, Y., Zhang, C., and Shi, Q.: In-House Standard
612 Method for Molecular Characterization of Dissolved Organic Matter by FT-ICR
613 Mass Spectrometry, *ACS Omega*, 5, 11730-11736, 10.1021/acsomega.0c01055,
614 2020.

615 Hodas, N., Sullivan, A. P., Skog, K., Keutsch, F. N., Collett Jr, J. L., Decesari, S.,
616 Facchini, M. C., Carlton, A. G., Laaksonen, A., and Turpin, B. J.: Aerosol liquid
617 water driven by anthropogenic nitrate: Implications for lifetimes of water-
618 soluble organic gases and potential for secondary organic aerosol formation,
619 *Environ. Sci. Technol.*, 48, 11127-11136.

620 <https://doi.org/11110.11021/es5025096>, 2014.

621 Hu, W., Hu, M., Hu, W. W., Zheng, J., Chen, C., Wu, Y., and Guo, S.: Seasonal
622 variations in high time-resolved chemical compositions, sources, and evolution
623 of atmospheric submicron aerosols in the megacity Beijing, *Atmos. Chem.*
624 *Phys.*, 17, 9979-10000, 10.5194/acp-17-9979-2017, 2017.

625 Koch, B. P. and Dittmar, T.: From mass to structure: an aromaticity index for high-
626 resolution mass data of natural organic matter, *Rapid Commun. Mass Spectrom.*,
627 20, 926-932, <https://doi.org/10.1002/rcm.2386>, 2006.

628 Kroll, J. H., Donahue, N. M., Jimenez, J. L., Kessler, S. H., Canagaratna, M. R., Wilson,
629 K. R., Altieri, K. E., Mazzoleni, L. R., Wozniak, A. S., Bluhm, H., Mysak, E. R.,
630 Smith, J. D., Kolb, C. E., and Worsnop, D. R.: Carbon oxidation state as a metric
631 for describing the chemistry of atmospheric organic aerosol, *Nat. Chem.*, 3, 133-
632 139, 10.1038/nchem.948, 2011.

633 Künzli, N., Kaiser, R., Medina, S., Studnicka, M., Chanel, O., Filliger, P., Herry, M.,
634 Horak, F., Jr., Puybonnieux-Textier, V., Quénel, P., Schneider, J., Seethaler, R.,
635 Vergnaud, J. C., and Sommer, H.: Public-health impact of outdoor and traffic-
636 related air pollution: a European assessment, *Lancet (London, England)*, 356,
637 795-801, 10.1016/s0140-6736(00)02653-2, 2000.

638 Lee, B. H., Mohr, C., Lopez-Hilfiker, F. D., Lutz, A., Hallquist, M., Lee, L., Romer, P.,
639 Cohen, R. C., Iyer, S., Kurtén, T., Hu, W., Day, D. A., Campuzano-Jost, P.,
640 Jimenez, J. L., Xu, L., Ng, N. L., Guo, H., Weber, R. J., Wild, R. J., Brown, S.
641 S., Koss, A., Gouw, J. d., Olson, K., Goldstein, A. H., Seco, R., Kim, S., McAvey,

642 K., Shepson, P. B., Starn, T., Baumann, K., Edgerton, E. S., Liu, J., Shilling, J.
643 E., Miller, D. O., Brune, W., Schobesberger, S., D'Ambro, E. L., and Thornton,
644 J. A.: Highly functionalized organic nitrates in the southeast United States:
645 Contribution to secondary organic aerosol and reactive nitrogen budgets, *P. Natl.*
646 *Acad. Sci. U. S. A.*, 113, 1516-1521, doi:10.1073/pnas.1508108113, 2016.

647 Li, W., Teng, X., Chen, X., Liu, L., Xu, L., Zhang, J., Wang, Y., Zhang, Y., and Shi, Z.:
648 Organic Coating Reduces Hygroscopic Growth of Phase-Separated Aerosol
649 Particles, *Environmental Science & Technology*, 55, 16339-16346,
650 10.1021/acs.est.1c05901, 2021a.

651 Li, X., Song, S., Zhou, W., Hao, J., Worsnop, D., and Jiang, J.: Interactions between
652 aerosol organic components and liquid water content during haze episodes in
653 Beijing, *Atmos. Chem. Phys.*, 19, 12163-12174, 10.5194/acp-19-12163-2019,
654 2019.

655 Li, X., Zhang, Y., Shi, L., Kawamura, K., Kunwar, B., Takami, A., Arakaki, T., and Lai,
656 S.: Aerosol Proteinaceous Matter in Coastal Okinawa, Japan: Influence of Long-
657 Range Transport and Photochemical Degradation, *Environmental Science &*
658 *Technology*, 56, 5256-5265, 10.1021/acs.est.1c08658, 2022.

659 Li, Y., Zhao, J., Wang, Y., Seinfeld, J. H., and Zhang, R.: Multigeneration Production
660 of Secondary Organic Aerosol from Toluene Photooxidation, *Environ. Sci.*
661 *Technol.*, 55, 8592-8603, 10.1021/acs.est.1c02026, 2021b.

662 Lin, P., Liu, J., Shilling, J. E., Kathmann, S. M., Laskin, J., and Laskin, A.: Molecular
663 characterization of brown carbon (BrC) chromophores in secondary organic

664 aerosol generated from photo-oxidation of toluene, *Phys. Chem. Chem. Phys.*,
665 17, 23312-23325, 10.1039/C5CP02563J, 2015.

666 Lv, S., Wang, F., Wu, C., Chen, Y., Liu, S., Zhang, S., Li, D., Du, W., Zhang, F., Wang,
667 H., Huang, C., Fu, Q., Duan, Y., and Wang, G.: Gas-to-Aerosol Phase
668 Partitioning of Atmospheric Water-Soluble Organic Compounds at a Rural Site
669 in China: An Enhancing Effect of NH₃ on SOA Formation, *Environ. Sci.*
670 *Technol.*, 56, 3915-3924, 10.1021/acs.est.1c06855, 2022.

671 Ma, W., Zheng, F., Zhang, Y., Chen, X., Zhan, J., Hua, C., Song, B., Wang, Z., Xie, J.,
672 Yan, C., Kulmala, M., and Liu, Y.: Weakened Gas-to-Particle Partitioning of
673 Oxygenated Organic Molecules in Liquified Aerosol Particles, *Environmental*
674 *Science & Technology Letters*, 10.1021/acs.estlett.2c00556, 2022.

675 Mozurkewich, M.: The dissociation constant of ammonium nitrate and its dependence
676 on temperature, relative humidity and particle size, *Atmos. Environ.*, 27, 261-
677 270, [https://doi.org/10.1016/0960-1686\(93\)90356-4](https://doi.org/10.1016/0960-1686(93)90356-4), 1993.

678 Müller, A., Miyazaki, Y., Tachibana, E., Kawamura, K., and Hiura, T.: Evidence of a
679 reduction in cloud condensation nuclei activity of water-soluble aerosols caused
680 by biogenic emissions in a cool-temperate forest, *Sci. Rep.*, 7, 8452. DOI:
681 8410.1038/s41598-41017-08112-41599., 2017.

682 Nguyen, T. K. V., Capps, S. L., and Carlton, A. G.: Decreasing Aerosol Water Is
683 Consistent with OC Trends in the Southeast U.S, *Environ. Sci. Technol.*, 49,
684 7843-7850. <https://doi.org/10.1021/acs.est.7845b00828>, 2015.

685 Nguyen, T. K. V., Zhang, Q., Jimenez, J. L., Pike, M., and Carlton, A. G.: Liquid water:

686 ubiquitous contributor to aerosol mass, *Environ. Sci. Tech. Lett.*, 3, 257-263.
687 <https://doi.org/210.1021/acs.estlett.1026b00167>, 2016.

688 Qiao, W., Guo, H., He, C., Shi, Q., Xiu, W., and Zhao, B.: Molecular Evidence of
689 Arsenic Mobility Linked to Biodegradable Organic Matter, *Environ. Sci.*
690 *Technol.*, 54, 7280-7290. <https://doi.org/210.1021/acs.est.7280c00737>, 2020.

691 Qiu, Y., Xie, Q., Wang, J., Xu, W., Li, L., Wang, Q., Zhao, J., Chen, Y., Chen, Y., Wu,
692 Y., Du, W., Zhou, W., Lee, J., Zhao, C., Ge, X., Fu, P., Wang, Z., Worsnop, D.
693 R., and Sun, Y.: Vertical Characterization and Source Apportionment of Water-
694 Soluble Organic Aerosol with High-resolution Aerosol Mass Spectrometry in
695 Beijing, China, *ACS Earth Space Chem.*, 3, 273-284,
696 [10.1021/acsearthspacechem.8b00155](https://doi.org/10.1021/acsearthspacechem.8b00155), 2019.

697 Sareen, N., Schwier, A., Lathem, T., Nenes, A., and McNeill, V. F.: Surfactants from the
698 gas phase may promote cloud droplet formation, *P. Natl. Acad. Sci. U. S. A.*,
699 110, 2723-2728. <https://doi.org/2710.1073/pnas.1204838110>, 2013.

700 Sareen, N., Waxman, E. M., Turpin, B. J., Volkamer, R., and Carlton, A. G.: Potential
701 of aerosol liquid water to facilitate organic aerosol formation: assessing
702 knowledge gaps about precursors and partitioning, *Environ. Sci. Technol.*, 51,
703 3327-3335, 2017.

704 Schmidt, F., Koch, B. P., Goldhammer, T., Elvert, M., Witt, M., Lin, Y.-S., Wendt, J.,
705 Zabel, M., Heuer, V. B., and Hinrichs, K.-U.: Unraveling signatures of
706 biogeochemical processes and the depositional setting in the molecular
707 composition of pore water DOM across different marine environments,

708 Geochim. Cosmochim. Ac., 207, 57-80.
709 <https://doi.org/10.1016/j.gca.2017.1003.1005>, 2017.

710 Simon, H., Bhawe, P., Swall, J., Frank, N., and Malm, W.: Determining the spatial and
711 seasonal variability in OM/OC ratios across the US using multiple regression,
712 Atmos. Chem. Phys., 11, 2933-2949. [https://doi.org/2910.5194/acp-2911-2933-](https://doi.org/2910.5194/acp-2911-2933-2011)
713 2011, 2011.

714 Song, J., Li, M., Jiang, B., Wei, S., Fan, X., and Peng, P. a.: Molecular Characterization
715 of Water-Soluble Humic like Substances in Smoke Particles Emitted from
716 Combustion of Biomass Materials and Coal Using Ultrahigh-Resolution
717 Electrospray Ionization Fourier Transform Ion Cyclotron Resonance Mass
718 Spectrometry, Environ. Sci. Technol., 52, 2575-2585, [10.1021/acs.est.7b06126](https://doi.org/10.1021/acs.est.7b06126),
719 2018.

720 Su, S., Xie, Q., Lang, Y., Cao, D., Xu, Y., Chen, J., Chen, S., Hu, W., Qi, Y., Pan, X.,
721 Sun, Y., Wang, Z., Liu, C.-Q., Jiang, G., and Fu, P.: High Molecular Diversity
722 of Organic Nitrogen in Urban Snow in North China, Environ. Sci. Technol.,
723 [10.1021/acs.est.0c06851](https://doi.org/10.1021/acs.est.0c06851), 2021.

724 Sun, Y., Du, W., Fu, P., Wang, Q., Li, J., ge, X., Zhang, q., Zhu, C., Ren, L., Xu, W.,
725 Zhao, J., Han, T., Worsnop, D., and Wang, Z.: Primary and secondary aerosols
726 in Beijing in winter: Sources, variations and processes, Atmos. Chem. Phys., 16,
727 8309-8329, [10.5194/acp-16-8309-2016](https://doi.org/10.5194/acp-16-8309-2016), 2016.

728 Tan, H., Cai, M., Fan, Q., Liu, L., Li, F., Chan, P. W., Deng, X., and Wu, D.: An analysis
729 of aerosol liquid water content and related impact factors in Pearl River Delta,

730 Sci. Total Environ., 579, 1822-1830.
731 <https://doi.org/10.1016/j.scitotenv.2016.1811.1167>, 2017.

732 Tong, H., Kourtchev, I., Pant, P., Keyte, I., O'Connor, I. P., Wenger, J., Pope, F., Harrison,
733 R., and Kalberer, M.: Molecular composition of organic aerosols at urban
734 background and road tunnel sites using ultra-high resolution mass spectrometry,
735 Faraday Discuss., 189, 51-68, 10.17863/CAM.5910, 2016.

736 Ushijima, S. B., Huynh, E., Davis, R. D., and Tolbert, M. A.: Seeded Crystal Growth of
737 Internally Mixed Organic–Inorganic Aerosols: Impact of Organic Phase State,
738 The Journal of Physical Chemistry A, 125, 8668-8679,
739 10.1021/acs.jpca.1c04471, 2021.

740 Wang, J., Gui, H., Yang, Z., Yu, T., Zhang, X., and Liu, J.: Real-world gaseous emission
741 characteristics of natural gas heavy-duty sanitation trucks, J. Environ. Sci., 115,
742 319-329, <https://doi.org/10.1016/j.jes.2021.06.023>, 2022.

743 Wang, J., Ye, J., Zhang, Q., Zhao, J., Wu, Y., Li, J., Liu, D., Li, W., Zhang, Y., Wu, C.,
744 Xie, C., Qin, Y., Lei, Y., Huang, X., Guo, J., Liu, P., Fu, P., Li, Y., Lee, H. C.,
745 Choi, H., Zhang, J., Liao, H., Chen, M., Sun, Y., Ge, X., Martin, S. T., and Jacob,
746 D. J.: Aqueous production of secondary organic aerosol from fossil-fuel
747 emissions in winter Beijing haze, Proceedings of the National Academy of
748 Sciences, 118, e2022179118, 10.1073/pnas.2022179118, 2021.

749 Xie, Q., Sihui, S., Chen, S., Xu, Y., Cao, D., Chen, J., Ren, L., Yue, S., Zhao, W., Sun,
750 Y., Wang, Z., Tong, H., Su, H., Cheng, Y., Kawamura, K., Jiang, G., Liu, C.-Q.,
751 and Fu, P.: Molecular characterization of firework-related urban aerosols using

752 Fourier transform ion cyclotron resonance mass spectrometry, *Atmos. Chem.*
753 *Phys.*, 20, 6803-6820, 10.5194/acp-20-6803-2020, 2020.

754 Xu, Y., Wu, D. S., Xiao, H. Y., and Zhou, J. X.: Dissolved hydrolyzed amino acids in
755 precipitation in suburban Guiyang, southwestern China: Seasonal variations and
756 potential atmospheric processes, *Atmos. Environ.*, 211, 247-255.
757 <https://doi.org/210.1016/j.atmosenv.2019.1005.1011>, 2019.

758 Xu, Y., Xiao, H., Wu, D., and Long, C.: Abiotic and Biological Degradation of
759 Atmospheric Proteinaceous Matter Can Contribute Significantly to Dissolved
760 Amino Acids in Wet Deposition, *Environ. Sci. Technol.*, 54, 6551-6561.
761 <https://doi.org/6510.1021/acs.est.6550c00421>, 2020a.

762 Xu, Y., Dong, X.-N., Xiao, H.-Y., Zhou, J.-X., and Wu, D.-S.: Proteinaceous Matter and
763 Liquid Water in Fine Aerosols in Nanchang, Eastern China: Seasonal Variations,
764 Sources, and Potential Connections, *J. Geophys. Res.: Atmos.*, 127,
765 e2022JD036589. <https://doi.org/036510.031029/032022JD036589>, 2022.

766 Xu, Y., Miyazaki, Y., Tachibana, E., Sato, K., Ramasamy, S., Mochizuki, T., Sadanaga,
767 Y., Nakashima, Y., Sakamoto, Y., Matsuda, K., and Kajii, Y.: Aerosol Liquid
768 Water Promotes the Formation of Water-Soluble Organic Nitrogen in
769 Submicrometer Aerosols in a Suburban Forest, *Environ. Sci. Technol.*, 54,
770 1406-1414. <https://doi.org/1410.1021/acs.est.1409b05849>, 2020b.

771 Yang, D., Zhu, S., Ma, Y., Zhou, L., Zheng, F., Wang, L., Jiang, J., and Zheng, J.:
772 Emissions of Ammonia and Other Nitrogen-Containing Volatile Organic
773 Compounds from Motor Vehicles under Low-Speed Driving Conditions,

774 Environ. Sci. Technol., 56, 5440-5447, 10.1021/acs.est.2c00555, 2022.

775 Yeh, G. K. and Ziemann, P. J.: Alkyl Nitrate Formation from the Reactions of C8–C14
776 n-Alkanes with OH Radicals in the Presence of NO_x: Measured Yields with
777 Essential Corrections for Gas–Wall Partitioning, *J. Phys. Chem. A*, 118, 8147-
778 8157, 10.1021/jp500631v, 2014.

779 Yttri, K. E., Aas, W., Bjerke, A., Cape, J., Cavalli, F., Ceburnis, D., Dye, C., Emblico,
780 L., Facchini, M., and Forster, C.: Elemental and organic carbon in PM₁₀: a one
781 year measurement campaign within the European Monitoring and Evaluation
782 Programme EMEP, *Atmos. Chem. Phys.*, 7, 5711-5725.
783 <https://doi.org/5710.5194/acp-5717-5711-2007>, 2007.

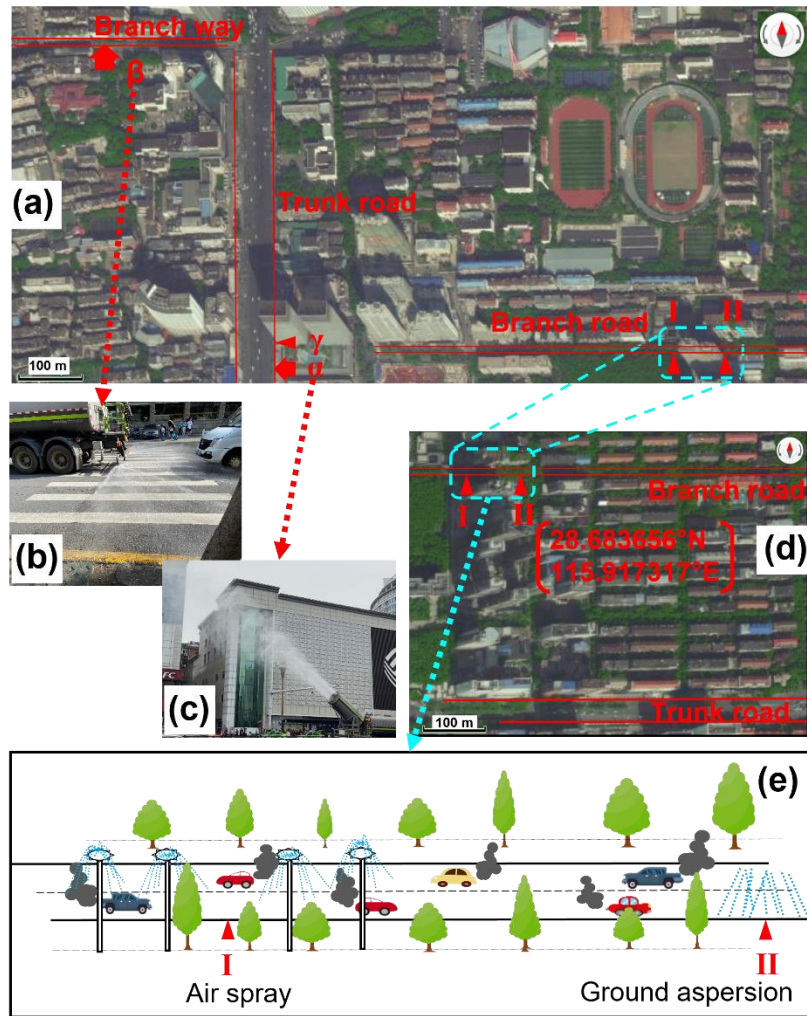
784 Yu, H., Li, W., Zhang, Y., Tunved, P., Dall'Osto, M., Shen, X., Sun, J., Zhang, X., Zhang,
785 J., and Shi, Z.: Organic coating on sulfate and soot particles during late summer
786 in the Svalbard Archipelago, *Atmos. Chem. Phys.*, 19, 10433-10446,
787 10.5194/acp-19-10433-2019, 2019.

788 Yue, H., He, C., Huang, Q., Yin, D., and Bryan, B. A.: Stronger policy required to
789 substantially reduce deaths from PM_{2.5} pollution in China, *Nat. Commun.*, 11,
790 1462, 10.1038/s41467-020-15319-4, 2020.

791

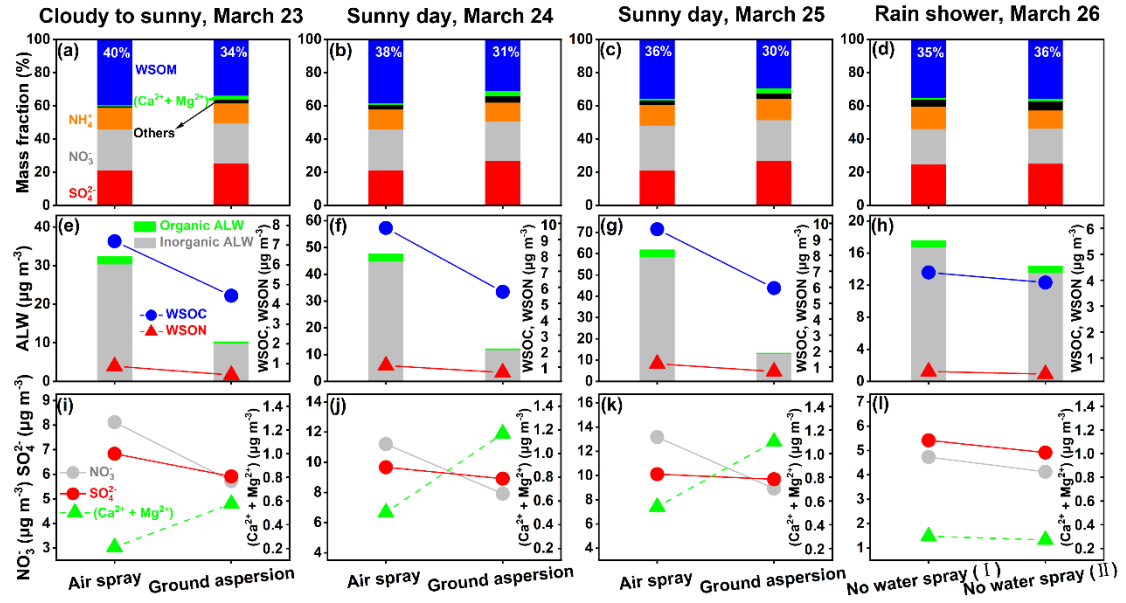
Table 1. The number of compounds in different subgroups in different samples and the number fractions of common molecules in the same subgroup in different samples.

Sample type (Date: Mar. 23–26)	Total	CHO	Common (CHO)	Common fraction (CHO)	CHON	Common (CHON)	Common fraction (CHON)
Air spray (23)	7069	1766		63%	2375		55%
Ground aspersion (23)	6166	1233	1104	90%	1803	1308	73%
Air spray (24)	7317	1861		53%	2447		50%
Ground aspersion (24)	6067	1098	990	90%	1501	1225	82%
Air spray (25)	8102	2037		39%	2685		45%
Ground aspersion (25)	5966	845	804	95%	1464	1209	83%
No water spray (I) (26)	6998	1621		81%	2120		74%
No water spray (II) (26)	6990	1539	1315	85%	1963	1579	80%



1
2
3
4
5
6
7
8
9
10

Figure 1. Map (Baidu, China) showing (a) the study area. The symbol of “ γ ” indicates the location where $PM_{2.5}$ mass concentration was monitored. The symbols of “ α ” and “ β ” refer to the locations where (b) the mist cannon truck photograph and (c) the traditional sprinkling truck photograph were taken, respectively. The symbol of “I” indicates that (d) the sampling was conducted on the air spray road segment or no water spray road segment (I). The symbol of “II” indicates that (d) the sampling was conducted on the ground aspersion road segment or no water spray road segment (II). Figure (e) shows the conceptual diagram of the sampling campaign.

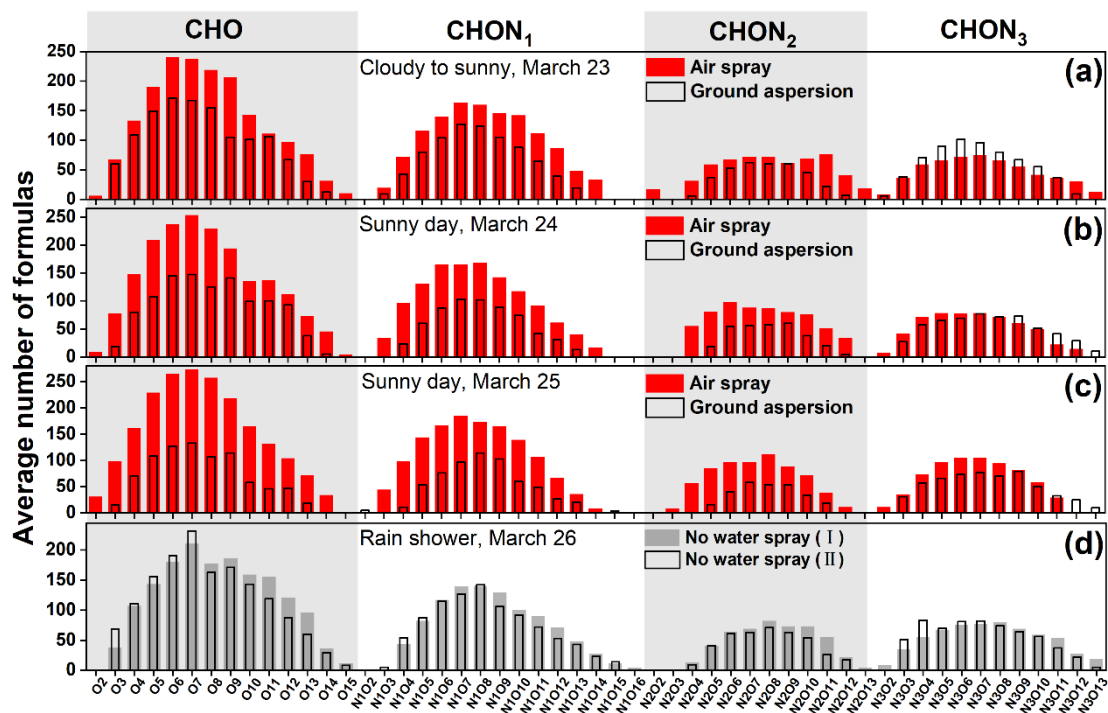


11

12 **Figure 2.** The mass fractions of chemical components in $\text{PM}_{2.5}$: (a, b, c) air spray vs
 13 ground aspersion and (d) no water spray (I) vs no water spray (II). The mass
 14 concentrations of ALW, WSOC, and WSON in $\text{PM}_{2.5}$: (e, f, g) air spray vs ground
 15 aspersion and (h) no water spray (I) vs no water spray (II). The mass concentrations of
 16 NO_3^- and SO_4^{2-} , as well as the sum of Ca^{2+} and Mg^{2+} concentrations in $\text{PM}_{2.5}$: (i, j, k)
 17 air spray vs ground aspersion and (l) no water spray (I) vs no water spray (II).

18

19



20

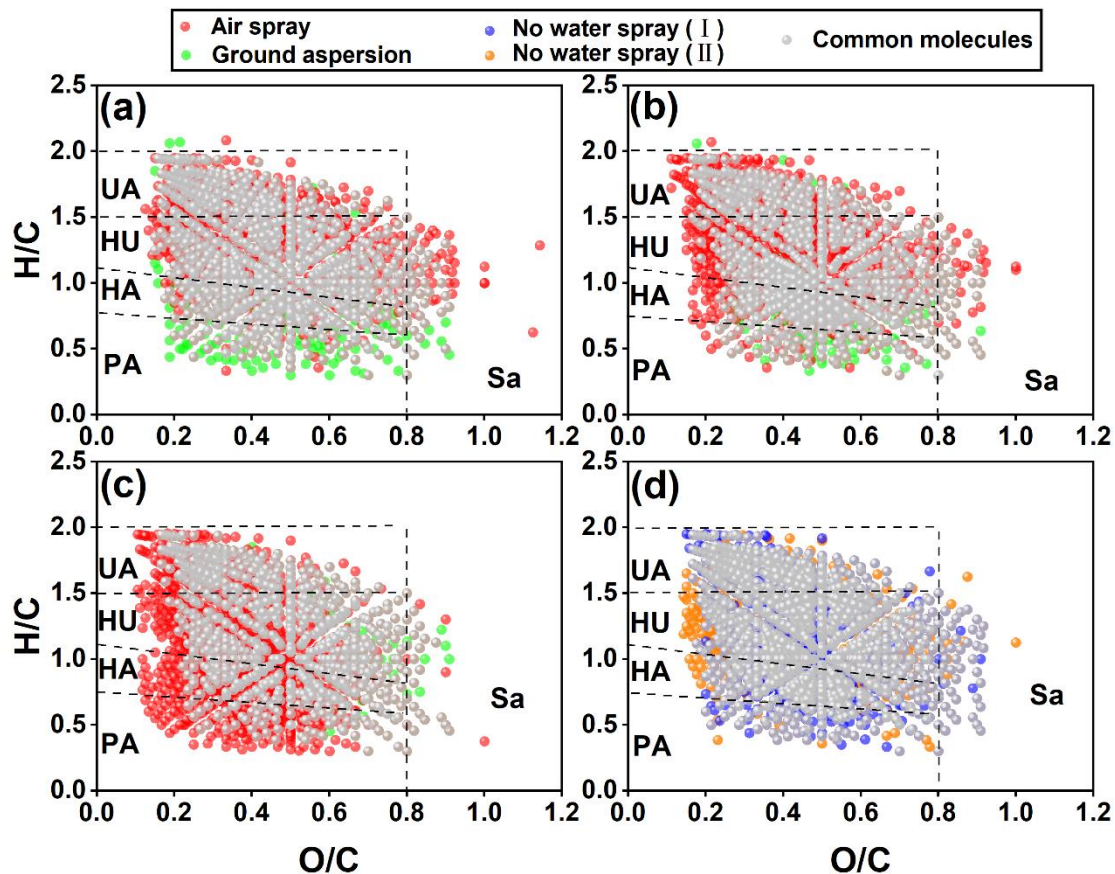
21 **Figure 3.** Classification of CHO and CHON species into subgroups according to the

22 number of O atoms in their molecules in WSOM in PM_{2.5} collected from different cases:

23 (a, b, c) air spray vs ground aspersion and (d) no water spray (I) vs no water spray (II).

24

25

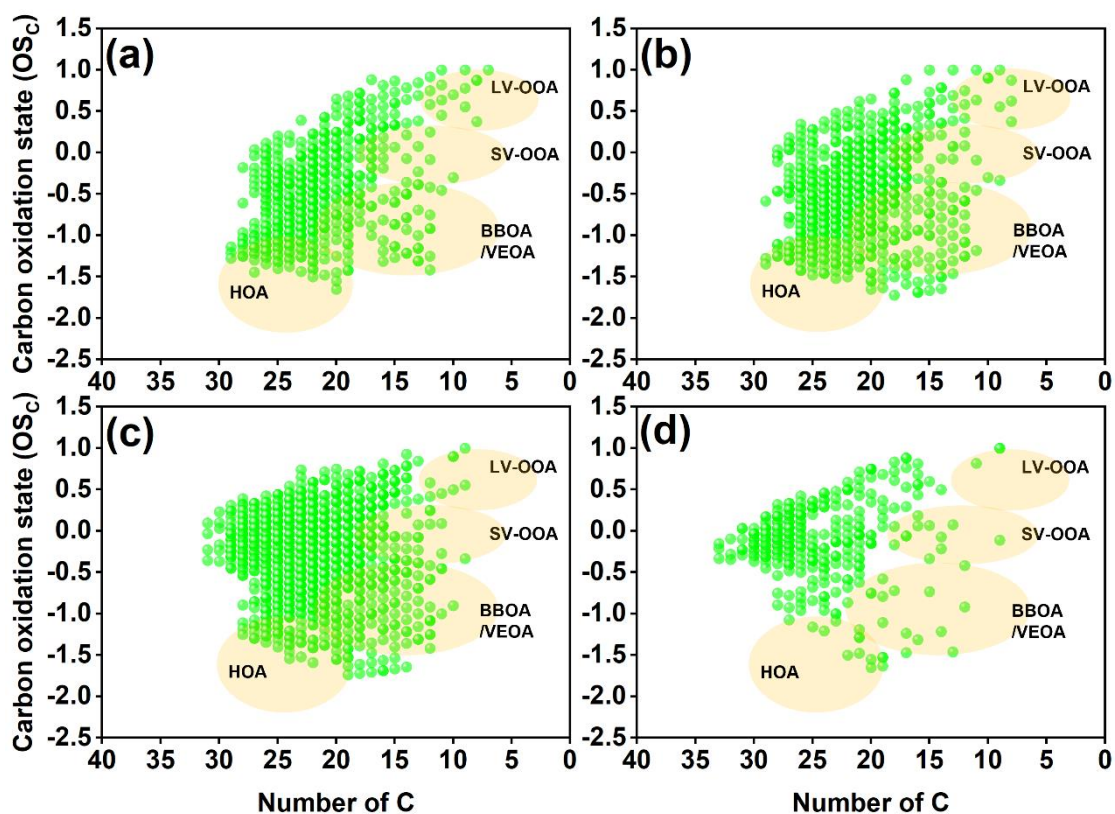


27

28 **Figure 4.** Van Krevelen diagrams of CHO compounds in WSOM in PM_{2.5} collected
 29 from different cases: air spray vs ground aspersion on (a) March 23, (b) March 24, and
 30 (c) March 25 and two road segments without water spray (I vs II) on (d) March 26. The
 31 classifications of compounds include unsaturated aliphatic-like (UA), highly
 32 unsaturated-like (HU), highly aromatic-like (HA), polycyclic aromatic-like (PA), and
 33 saturated-like (Sa) molecules.

34

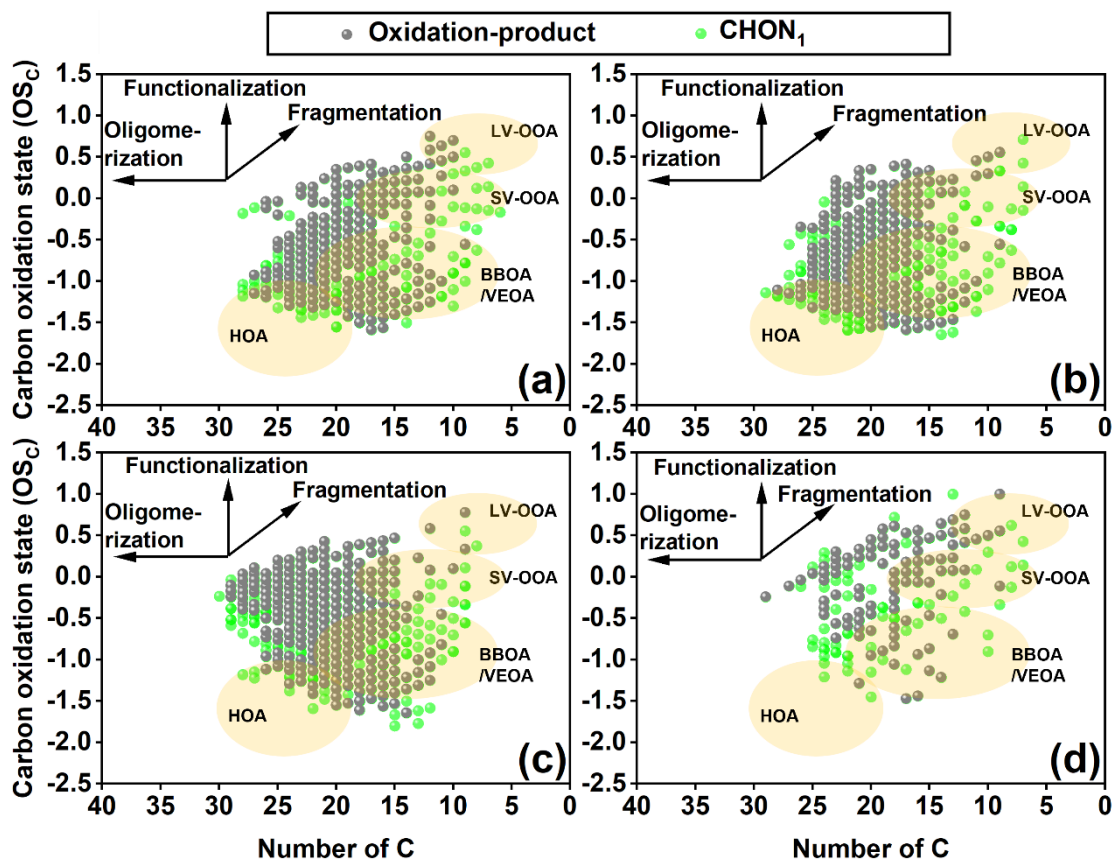
35



36

37 **Figure 5.** OS_C of unique CHO molecules in WSOM in $PM_{2.5}$ collected from different
 38 cases: air spray vs ground aspersion on (a) March 23, (b) March 24, and (c) March 25
 39 and two road segments without water spray (I vs II) on (d) March 26. For the above
 40 comparative cases, the unique CHO compounds indicate the CHO molecules identified
 41 in $PM_{2.5}$ collected from the air spray (/no water spray-I) road segments. The light orange
 42 background represents areas of HOA (hydrocarbon-like organic aerosol), BBOA and
 43 VEOA (biomass burning and vehicle emission organic aerosols) (Kroll et al., 2011;
 44 Tong et al., 2016), SV-OOA (semivolatile oxidized organic aerosol), and LV-OOA (low-
 45 volatility oxidized organic aerosol) (Kroll et al., 2011).

46

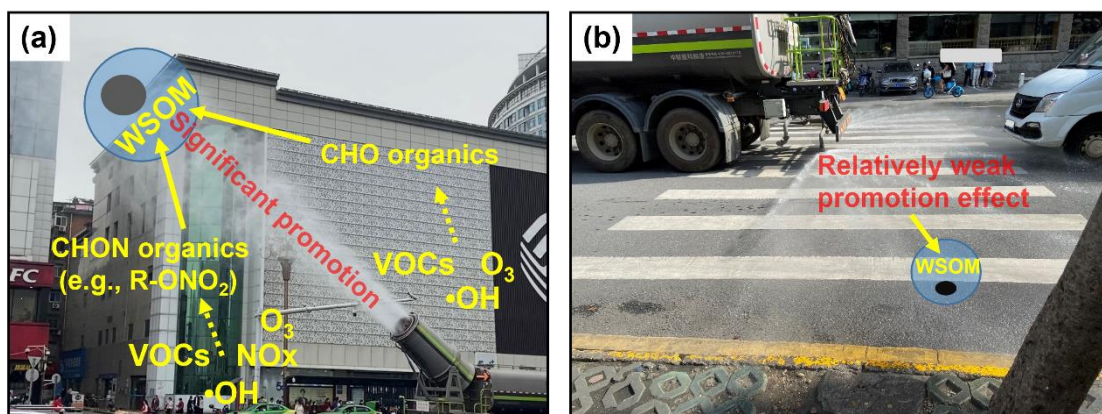


47

48 **Figure 6.** OS_C of unique $CHON_1$ molecules in WSOM in $PM_{2.5}$ collected from different
 49 cases: air spray vs ground aspersion on (a) March 23, (b) March 24, and (c) March 25
 50 and two road segments without water spray (I vs II) on (d) March 26. For the above
 51 comparative cases, the unique $CHON_1$ compounds indicate the $CHON_1$ molecules
 52 identified in $PM_{2.5}$ collected from the air spray (/no water spray-I) road segments. The
 53 light orange background represents areas of HOA, BBOA and VEOA, SV-OOA, and
 54 LV-OOA. The grey circles refer to the identified oxidation-product pairs.

55

56



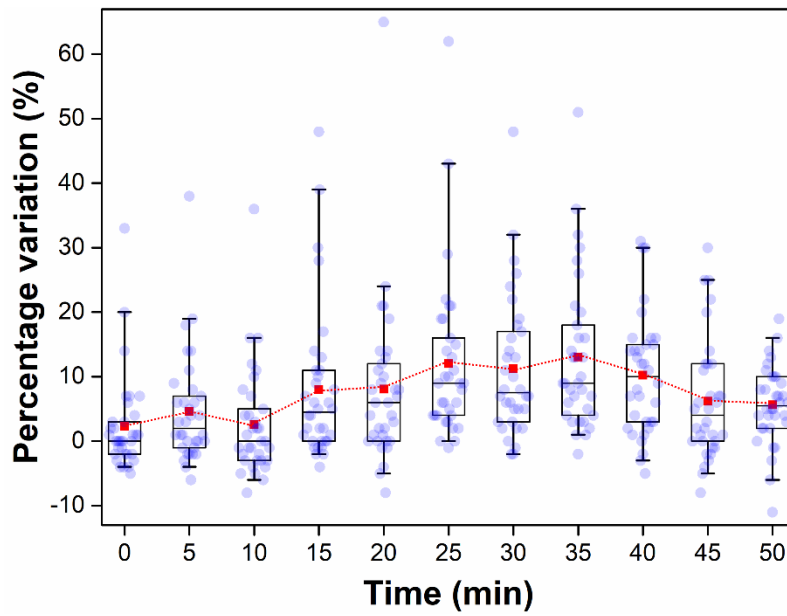
57

58 **Figure 7.** Conceptual picture showing the influence of (a) mist cannon truck and (b)
 59 traditional sprinkling truck on water-soluble organic matter (WSOM) formation in the
 60 urban road environment.

61

62

63



64

65 **Figure 8.** The time series of percentage variations in PM_{2.5} mass concentrations after
66 mist cannon truck operation ($n = 34$). Each box encompasses the 25th–75th percentiles.
67 Whiskers are the 5th and 95th percentiles. The solid lines and squares inside boxes
68 indicate the median and mean. All individual data are presented as circles.

69